

Received March 19, 2019, accepted April 8, 2019, date of publication April 22, 2019, date of current version May 20, 2019.

Digital Object Identifier 10.1109/ACCESS.2019.2912004

A Fully Distributed Voltage Optimization Method for Distribution Networks Considering Integer Constraints of Step Voltage Regulators

YIXIN LIU¹, LI GUO¹, (Member, IEEE), CHANG LU¹, YUANYUAN CHAI¹, SHUANG GAO¹, (Member, IEEE), AND BIN XU²

¹Key Laboratory of Smart Grid, Ministry of Education, Tianjin University, Tianjin 300072, China

²Institute of Electric Power Research, Hefei 230002, China

Corresponding author: Li Guo (liguo@tju.edu.cn)

This work was supported by the National Key Technology Research and Development Program of China under Grant 2016YFB0900400.

ABSTRACT With the increasing penetration of distributed photovoltaics (PVs), the operation and control of distribution networks (DNs), especially voltage control, have become more complicated. To deal with the voltage violation problem caused by large-scale PV access, this paper presents a fully distributed optimization method that combines the alternative direction multiplier method (ADMM) with the branch and bound method (BBM) for regional DNs. The total cost of active power losses and PV generation losses is minimized by making full use of the voltage regulation resources, e.g., reactive power compensators, step voltage regulators (SVR), and PV inverters, and the ADMM is employed to realize the intra-regional optimization and inter-regional coordination. To overcome the non-convex problem that is introduced by the SVR, the constraints of real-value tap positions are reformulated as linear inequality constraints of boundary voltages and added to the original problem, then the integer optimal solutions of SVR tap positions are obtained by BBM. The effectiveness of the proposed method is verified via numerical simulations on a practical 32-bus DN in China and a modified IEEE123-bus system.

INDEX TERMS Active distribution networks, distributed optimization, voltage control, step voltage regulator.

NOMENCLATURE

ACRONYMS

DN	Distribution network
PV	Photovoltaic generator
RPC	Reactive power compensator
SVR	Step voltage regulator

INDICES AND SETS

i, j	Indices of nodes in DN
a, b, c, d	Indices of boundary nodes in each region
n	Index of regions, from 1 to R
k	Iteration index for distributed calculation
k	Iteration index for distributed calculation
N	Set of nodes in DN
N_B	Set of boundary nodes in all regions
R_n	Set of boundary nodes in region n
L_B	Set of inter-regional interconnected lines

The associate editor coordinating the review of this manuscript and approving it for publication was Peng-Yong Kong.

VARIABLES

$P_{dec,j}$	Active power curtailment amount of PV units at node j
$Q_{G,j}$	Reactive power generated by PV units at node j
$Q_{C,j}$	Reactive power generated by RPC at node j
I_{ij}, l_{ij}	Current amplitude flowing from node i to node j and its square
U_j	Voltage amplitude of node j
P_{ij}, Q_{ij}	Active and reactive power flowing from node i to node j
P_j, Q_j	Active and reactive power of net loads at node j
g	SVR tap position
P_{ab}^*, Q_{ab}^*	Transmission active and reactive power of branch ab , regarded as virtual load for upstream region, $\forall ab \in L_B$
P_{ab}, Q_{ab}	Transmission active and reactive power of branch ab , $\forall ab \in L_B$

VECTORS

\mathbf{y}, \mathbf{z}	Global variable vectors of transmission active and reactive power between regions
$\lambda^P/\lambda^{P^*}/\lambda^Q/\lambda^{Q^*}$	Lagrange multiplier vectors corresponding to equality constraints of transmission active and reactive power between regions
\mathbf{r}, \mathbf{s}	Primal residual and dual residual vectors

PARAMETERS

$P_{L,l}^{\max}, Q_{L,l}^{\max}$	Active and reactive power of full load
r_0, x_0	Resistance and reactance per unit length
ΔU^{\max}	Maximum allowed voltage loss rate
π_{PV}	Unit power generation revenue of PV, including government subsidies
π_P	Unit on-grid price
R_{ij}, X_{ij}	Resistance and reactance of branch ij
$P_{L,j}, Q_{L,j}$	Active and reactive power of loads at node j
U^{\max}, U^{\min}	Upper bound and lower bound of voltage amplitude
$Q_{C,j}^{\max}, Q_{C,j}^{\min}$	Upper and lower bound of the reactive power generated by RPC at node j
$S_{G,j}$	Installation capacity of PVs inverter at node j
d_{step}	Adjustment amount per tap position of SVR
ρ	Penalty parameter
δ_d	Predefined threshold for iterative termination of ADMM

I. INTRODUCTION

With the increasing penetration of distributed photovoltaics (PVs), distribution networks (DNs) are gradually transforming from passive networks with unidirectional power flow to active distribution networks (ADNs) with bidirectional power flow [1]. The reverse power flow and voltage violation caused by excess PV power have brought significant challenges to the operational stability of DNs, and thus the optimization approach for ADNs to deal with these problems has become a hot topic of research in recent years [2]–[4].

The voltage optimization of ADNs is typically formulated as a mixed-integer non-linear optimization problem (MINOP) as it includes both continuous and discrete decision variables, e.g. the scheduling power of reactive power compensators (RPCs), distributed generators (DGs) and tap positions of step voltage regulator (SVR). Many approaches have been proposed to solve the MINOP, including artificial intelligence algorithms and mathematical programming methods. In [5], a hybrid particle swarm optimization (HPSO) method is proposed to deal with the reconfiguration problem of DNs coupled with reactive power control of DGs, and the fuzzy adaptive inference is integrated into HPSO to avoid being trapped in local optima. Reference [6] develops a genetic algorithm for the joint

optimization of network reconfiguration and capacitor control. Taking into account the control of capacitor banks, voltage regulators, and under-load tap changers (ULTCs), a mixed-integer quadratically constrained programming problem is formulated in [7] to achieve the goals of loss reduction and voltage profile improvement etc. Reference [8] proposes a mixed-integer second-order cone programming (MISOCP) relaxation approach for the AC optimal transmission switching problem, and Reference [9] combines VAR optimization with network reconfiguration and converts it to a MISOCP.

The abovementioned literatures show greater loss reduction and better voltage profiles through comprehensive coordination of RPCs, voltage regulators and network reconfiguration, whereas the problems are formulated in a centralized manner, which are however, expected to encounter significant technical challenges, e.g. communication bottleneck for incremental data volume caused by large-scale integration of DGs, weak robustness for cyber-physical system failure, and expensive communication costs to solve the centralized optimization problems [10]. Considering these significant challenges, a fully distributed optimization algorithm for ADNs is preferred, which only requires local and adjacent areas' information and can achieve the goal of global optimum by coordinating iteration among regions.

The key points of distributed optimization algorithm for ADNs lie in two aspects: optimization within a region and inter-regional coordination. For the regional scheduling, the optimization problem is essentially nonconvex and NP-hard due to the quadratic relationship between voltage and power injection, etc. and may not converge when solving it directly by distributed algorithm. Therefore, many convexification techniques have been proposed to overcome this restriction. The LinDistFlow is applied to approximate the original nonlinear power flow constraints and make the problem convex in [11], but the accuracy is not satisfactory in some application scenarios, especially for ADNs. To compensate the approximation error of the LinDistFlow equation, the boundary data is updated after parallel optimization by power flow calculation in each region in [12]. The semi-definite relaxation (SDR) and second-order cone relaxation (SOCR) are also employed to relax the original nonconvex problem in [13], [14] and [8]–[10], [15], respectively. However, SDR involves additional large-scale variables and may not appropriate for ADNs with large number of PV access. The accuracy condition of SOCR is satisfied when the objective is strictly increasing in branch current [16]. For DNs with high penetration of distributed PV, however, this may result in undesirable loss of PV power generation, as the accuracy condition is no longer satisfied when taking the PV curtailment minimization as a part of the objective. Faced with various optimization goals in practice, it is necessary to improve the conic relaxation to obtain an effective solution, e.g. adding increasingly tight cutting planes [17] or leaf branch current cut [18] into the constraints. The inter-regional coordination can be transformed into an optimization

problem with equality consistency constraints. Existing algorithms can basically be classified into three categories according to the way of dealing with consistency constraints: the primal domain algorithm [19]–[22], the dual domain algorithm [23], [24], and the primal-dual algorithm [25]–[27]. The alternative direction multiplier method (ADMM), as a promising distributed algorithm for ADNs optimization, is a typical dual domain algorithm, whose equality consistency constraints are satisfied by dual iterations. The literatures [10]–[12] and [14] apply SOCR, LinDistFlow approximation and SDR to relax power flow equations before using ADMM, respectively. These literatures mainly focus on continuous variables, whereas discrete variables, such as SVR tap positions, are not considered. Actually, in the over-voltage scenario caused by redundant PV power, SVR can lower the feeder voltage and avoid the PV active power curtailment (APC). In addition, SVR can improve the feeder voltage in the low voltage scenario, reducing the network losses. Unfortunately, taking SVR into consideration will introduce integer variables, i.e. the tap positions, into the optimization problem and make it nonconvex. As a result, the convergence condition of ADMM is no longer satisfied.

References	Power flow convexity method	Drawback	SVR
[10]	SOCR	Restricted relaxation accuracy (undesirable loss of PV power generation etc.)	/
[11]	LinDistflow	Insufficient accuracy for ADNs	/
[12]	LinDistflow with compensation	Accuracy is improved, but still need to be enhanced	/
[14]	SDR	Additional large-scale variables	/
Drawback: unable to deal with the problem with discrete variables			
↓ Consider SVR devices to increase the control flexibility			
How to solve the non-convex problem in a distributed manner ?			
↓			
Distributed optimization method that combines ADMM with BBM			

FIGURE 1. Comparisons with previous works related to distributed optimization of ADNs.

Fig. 1 summarizes the main drawbacks of previous works that using distributed algorithm to solve the voltage optimization of ADNs. As mentioned above, considering SVR devices can significantly improve the control flexibility and system benefits, but the nonconvexity introduced by SVR makes the distributed algorithm unable to converge. To solve this problem, a distributed optimization method that combines ADMM with branch and bound method (BBM) is proposed in this paper. The inter-regional coordination is realized via ADMM, and the nonconvexity introduced by SVR is handled through BBM. The main contributions of this paper are as follows.

1) A comprehensive optimal model that considers the scheduling of PV active and reactive power, RPCs and SVR is established. The relaxation problem (RP) of the original nonconvex problem is obtained by SOCR and cutting planes constraints. The voltage regulation resources are fully utilized

in the region, resulting in the reduction of undesirable loss of PV power.

2) The optimization of ADNs is conducted in a fully distributed manner. The inter-regional coordination, including the optimal real-value solution of SVR tap position, is solved by ADMM. Then, the tap constraint based on the real-value solution is transformed into linear inequality constraints of the regional boundary voltage and added to the RP. Finally, the optimal integer solution of SVR tap position is realized by BBM, disposing of the nonconvexity problem introduced by SVR.

The remainder of this paper is organized as follows: Section II describes the inter-regional coordination framework as well as the boundary interaction information. Section III detailed the intra-regional optimization model. ADMM and BBM are applied in Section IV to perform distributed inter-regional coordination. In Section V, the effectiveness of the proposed method is verified via numerical simulations on a practical 32-bus system in JinZhai, China and a modified IEEE123-bus system. Section VI outlines the main conclusions.

II. INTER-REGIONAL COORDINATION FRAMEWORK

The SVR is considered in this paper to provide flexible control means for various operation scenarios of the system. The installation position should take account the network topology and power flow distribution to ensure the nodal voltage within a predetermined range, especially the terminal nodes of long-feeder under full load condition. Therefore, we can employ the following formula to decide the installation position of SVR:

$$\frac{P_{L,l}^{\max} \cdot (r_0 l) + Q_{L,l}^{\max} \cdot (x_0 l)}{U_0 \cdot U_0} \leq \Delta U^{\max} \quad (1)$$

where $P_{L,l}^{\max}$ and $Q_{L,l}^{\max}$ represent the maximum active and reactive power under full load condition, respectively; U_0 is the feeder nominal voltage; l denotes the SVR installation point distance. The left term of (1) approximates the voltage drop before installation point of SVR and l should meet the following constraint according to (1):

$$l \leq \frac{\Delta U^{\max} \cdot U_0^2}{P_{L,l}^{\max} \cdot r_0 + Q_{L,l}^{\max} \cdot x_0} \quad (2)$$

The cluster control method has been proved to be an effective way to realize global optimization and overcome the technical challenges of centralized optimization for long-feeder DNs [28], [29]. A detailed cluster partition method that considers the voltage amplitude sensitivity with respect to active and reactive power is introduced in our previous work [12], based on which an inter-regional coordination framework is proposed in this paper, as illustrated in Fig. 2. It is worth noting that the distributed algorithm proposed in this paper is applicable for other cluster partition schemes that contain SVRs, here we employ this framework as an example to better describe our modeling process.

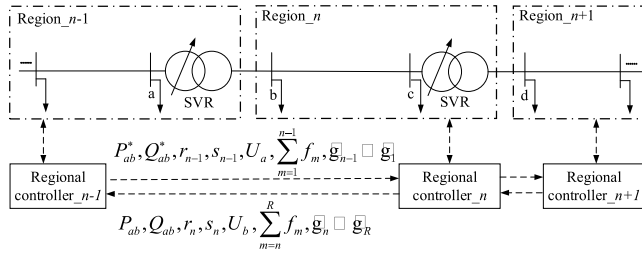


FIGURE 2. Inter-regional coordination framework.

Each region is equipped with a local controller to achieve intra-regional optimization and inter-regional coordination. For region $_n$ and its upstream region $_{n-1}$ ($n \geq 2$), the interactive information consists of the transmission active/reactive power of inter-regional interconnected lines (we define the transmission active/reactive power as virtual load from the view of upstream region and mark it with superscript *), the primal residual and dual residual of each region, the boundary node voltage, the objective function value of regional optimization problem and the real solution of SVR tap positions of each region. All these variables are related to ADMM and BBM and will be detailed explained in Section IV. The interactive process between regions is summarized as:

- 1) Each regional controller seeks for its optimal operation scheme in parallel and then transmits the transmission active/reactive power, the primal residual and dual residual to each other;
- 2) According to the received information, each regional controller performs a new round of intra-regional optimization until the primal residual and dual residual are reduced to a predefined threshold;
- 3) After the intra-regional optimization converges, regional controller $_{n-1}$ sends the boundary node voltage and the sum of the objective function value of itself and its upstream to regional controller $_n$, while regional controller $_n$ sends the boundary node voltage and the sum of the objective function value of itself and its downstream to regional controller $_{n-1}$;
- 4) Each regional controller calculates the real-value solution of SVR tap positions based on the voltage ratio. Then regional controller $_{n-1}$ sends the tap positions of itself and its upstream to regional controller $_n$, while regional controller $_n$ sends the tap positions of itself and its downstream to regional controller $_{n-1}$. Finally, BBM is applied to determine whether a branch is required based on the taps.

III. INTRA-REGIONAL OPTIMIZATION FORMULATION

A. ORIGINAL OPTIMIZATION MODEL

The regional controller is optimized in parallel to obtain the boundary data required for coordination between regions. The intra-regional optimization model is as follows:

1) OBJECTIVE FUNCTION

We aim to minimize the cost of network power losses and PV power generation losses in region n , which can be expressed as:

$$f_n = \min_{Q_{C,j}, P_{dec,j}, Q_{G,j}} \left(\pi_{PV} \sum_{j \in R_n} P_{dec,j} + \pi_P \sum_{j \in R_n, \forall i: i \rightarrow j} R_{ij} I_{ij}^2 \right) \quad (3)$$

where $Q_{C,j}$, $P_{dec,j}$, and $Q_{G,j}$ are the decision variables of the intra-regional optimization problem. The first term indicates the lost revenue due to APC of PV units; the second term denotes the active power losses cost of region n .

2) POWER FLOW EQUATIONS

$$\begin{cases} \sum_{i:i \rightarrow j} (P_{ij} - R_{ij} I_{ij}^2) - P_j = \sum_{o:j \rightarrow o} P_{jo} \\ \sum_{i:i \rightarrow j} (Q_{ij} - X_{ij} I_{ij}^2) - Q_j = \sum_{o:j \rightarrow o} Q_{jo} \\ U_j^2 = U_i^2 - 2(R_{ij} P_{ij} + X_{ij} Q_{ij}) + (R_{ij}^2 + X_{ij}^2) I_{ij}^2 \end{cases} \quad (4a)$$

and

$$\begin{cases} P_j = P_{L,j} - (P_{G,j}^{\max} - P_{dec,j}) \\ Q_j = Q_{L,j} - Q_{G,j} - Q_{C,j} \end{cases} \quad (4b)$$

$$I_{ij}^2 = \frac{P_{ij}^2 + Q_{ij}^2}{U_i^2} \quad (4c)$$

where $i \rightarrow j$ denotes the directional relation between node i and node j ; $P_{L,j}$ and $Q_{L,j}$ are the active and reactive power of loads at node j , including the active/reactive power of virtual loads; $P_{G,j}^{\max}$ represents the maximum active power generated by PV units under maximum power point tracking strategy.

3) NODAL VOLTAGE CONSTRAINT

The nodal voltage should meet the limits as:

$$U^{\min} \leq U_j \leq U^{\max} \quad (5)$$

where U^{\max} and U^{\min} are respectively the upper bound and lower bound of voltage amplitude.

4) PV UNITS AND RPC OPERATION CONSTRAINTS

Formula (6a) and (6b) denote the operation constraints of PV and RPC devices:

$$\begin{cases} 0 \leq P_{dec,j} \leq P_{G,j}^{\max} \\ Q_{G,j} \leq (P_{G,j}^{\max} - P_{dec,j}) \tan \theta \\ Q_{G,j}^2 \leq S_{G,j}^2 - (P_{G,j}^{\max} - P_{dec,j})^2 \end{cases} \quad (6a)$$

$$Q_{C,j}^{\min} \leq Q_{C,j} \leq Q_{C,j}^{\max} \quad (6b)$$

where $\theta = \cos^{-1} PF_{\min}$ is the power factor angle corresponding to the minimum power factor PF_{\min} .

B. CONVEX RELAXATION MODEL

The original optimization model (3)-(6) is nonconvex and cannot be directly solved by ADMM. The SOCR method is employed to transform it into a convex problem. Firstly, the voltage square term U_i^2 and the current square term I_{ij}^2 are replaced with u_i and l_{ij} , respectively. Then we have:

$$f_n = \min_{Q_{C,j}, P_{dec,j}, Q_{G,j}} \left(\pi_{PV} \sum_{j \in R_n} P_{dec,j} + \pi_P \sum_{j \in R_n, \forall i:i \rightarrow j} R_{ij} l_{ij} \right) \tag{7}$$

$$\begin{cases} \sum_{i:i \rightarrow j} (P_{ij} - R_{ij} l_{ij}) - P_j = \sum_{o:j \rightarrow o} P_{jo} \\ \sum_{i:i \rightarrow j} (Q_{ij} - X_{ij} l_{ij}) - Q_j = \sum_{o:j \rightarrow o} Q_{jo} \\ u_j = u_i - 2 (R_{ij} P_{ij} + X_{ij} Q_{ij}) + (R_{ij}^2 + X_{ij}^2) l_{ij} \end{cases} \tag{8}$$

$$l_{ij} = \frac{P_{ij}^2 + Q_{ij}^2}{u_i} \tag{9}$$

$$(U^{\min})^2 \leq u_j \leq (U^{\max})^2 \tag{10}$$

Due to the product of variables, (9) is still nonconvex and can be relaxed to the following form by SOCR:

$$\left\| \begin{matrix} 2P_{ij} \\ 2Q_{ij} \\ l_{ij} - u_i \end{matrix} \right\|_2 \leq l_{ij} + u_i \tag{11}$$

To deal with the problem that the relaxation accuracy of SOCR is insufficient under high PV penetration conditions, a cutting plane constraint formulated as (12a) is considered:

$$\sum_{i:i \rightarrow j} R_{ij} l_{ij} \leq \sum_{i:i \rightarrow j} R_{ij} L_{ij}^k \quad k \geq 1 \tag{12a}$$

and

$$L_{ij}^k = \frac{(P_{ij}^k)^2 + (Q_{ij}^k)^2}{u_i^k} \tag{12b}$$

where the superscript k represents the iterative counter of ADMM, which will be introduced in Section IV.

After the above process, the revised optimization model given by (4b), (6)-(8), (10)-(12) becomes a second-order cone programming model and can be solved quickly and accurately by convex optimization method.

IV. INTER-REGIONAL COORDINATION FORMULATION

A. ADMM FOR THE OPTIMAL POWER FLOW

The regional controller needs to achieve not only the optimal operation within its region, but also the coordination between regions. For the inter-regional coordination, the equality constraints of boundary node voltage and transmission power of interconnected lines should be considered, so that each region can carry out independent parallel optimization and ensure the convergence of inter-regional distributed optimization. As demonstrated in Fig. 1, SVR constraints between adjacent regions is expressed as (13a), and (13b) and (13c) correspond

to transmission power equation constraints between adjacent regions.

$$U_a = U_b (1 + g \cdot d_{step}) \tag{13a}$$

$$P_{ab}^* = y_{ab}, \quad y_{ab} = P_{ab} \quad \forall ab \in L_B \tag{13b}$$

$$Q_{ab}^* = z_{ab}, \quad z_{ab} = Q_{ab} \quad \forall ab \in L_B \tag{13c}$$

where y_{ab} and z_{ab} are the global variables of transmission active and reactive power of branch ab .

This paper applies ADMM to achieve distributed optimization between regions. Since the SVR constraint (13a) makes the problem nonconvex and does not satisfy the convergence condition of ADMM, we remove the constraint (13a) and ignore the boundary node voltage equation constraint firstly. Then the relaxation problem of the original problem, defined as RP, is obtained. ADMM algorithm guarantees the consistency equality constraints by dual iteration, so that the global optimal solution is obtained by coordinating the solution of the subproblems. Set $\lambda_{ab}^P, \lambda_{cd}^P, \lambda_{ab}^Q, \lambda_{cd}^Q$ as the Lagrange multipliers of transmission power equation constraints of adjacent regions, respectively. The augmented Lagrangian function of (7) can be revised as

$$\begin{aligned} L_n = f_n & + \sum_{ab \in L_B, b \in R_n} \left[\frac{\rho}{2} (y_{ab} - P_{ab})^2 + \lambda_{ab}^P (y_{ab} - P_{ab}) \right] \\ & + \sum_{cd \in L_B, c \in R_n} \left[\frac{\rho}{2} (P_{cd}^* - y_{cd})^2 + \lambda_{cd}^P (P_{cd}^* - y_{cd}) \right] \\ & + \sum_{ab \in L_B, b \in R_n} \left[\frac{\rho}{2} (z_{ab} - Q_{ab})^2 + \lambda_{ab}^Q (z_{ab} - Q_{ab}) \right] \\ & + \sum_{cd \in L_B, c \in R_n} \left[\frac{\rho}{2} (Q_{cd}^* - z_{cd})^2 + \lambda_{cd}^Q (Q_{cd}^* - z_{cd}) \right] \end{aligned} \tag{14}$$

where $\rho > 0$ is the penalty parameter, used to ensure the convergence of boundary data between adjacent regions.

The primal residual and dual residual are adopted to judge whether the solution process converges. The primal residual represents the deviation of boundary data between adjacent regions, and the dual residual indicates the vibration deviation of the regional boundary data in sequent iterations, which are formulated as:

$$\begin{aligned} r_n^{k+1} & = \sum_{\substack{ab \in L_B, b \in R_n \\ cd \in L_B, c \in R_n}} \left[\left| y_{ab}^{k+1} - P_{ab}^{k+1} \right| + \left| z_{ab}^{k+1} - Q_{ab}^{k+1} \right| \right. \\ & \quad \left. + \nu \left| y_{cd}^{k+1} - P_{cd}^{*,k+1} \right| + \left| z_{cd}^{k+1} - Q_{cd}^{*,k+1} \right| \right] \end{aligned} \tag{15}$$

$$\begin{aligned} s_n^{k+1} & = \sum_{\substack{ab \in L_B, b \in R_n \\ cd \in L_B, c \in R_n}} \left[\left| y_{ab}^{k+1} - y_{ab}^k \right| + \left| z_{ab}^{k+1} - z_{ab}^k \right| \right. \\ & \quad \left. + \left| y_{cd}^{k+1} - y_{cd}^k \right| + \left| z_{cd}^{k+1} - z_{cd}^k \right| \right] \end{aligned} \tag{16}$$

where r_n^{k+1} and s_n^{k+1} denote the primal residual and dual residual of region n at $k+1$ -th iteration, respectively. Define $\mathbf{r}^k := \{r_1^k, r_2^k \dots r_R^k\}^T$ and $\mathbf{s}^k := \{s_1^k, s_2^k \dots s_R^k\}^T$ as the column vectors composed of the primal residuals and dual residuals of all regions at k -th iteration.

The penalty parameter in (14) greatly affects the convergence speed. An excessively large penalty parameter will increase the dual residual, whereas the primal residual will increase if the penalty parameter is too small. Therefore, the penalty parameter of each region should be adjusted according to the relative size of the primal residual and dual residual [10]. When the dual residual is significantly larger than the primal residual, the penalty parameter needs to be reduced, and the parameter should be set larger when the primal residual is much larger than the dual residual, as given by (17).

$$\rho_n^{k+1} = \begin{cases} 0.5\rho_n^k, & \|s_n^{k+1}\|_2 \geq 10 \|r_n^{k+1}\|_2 \\ 2\rho_n^k, & \|r_n^{k+1}\|_2 \geq 10 \|s_n^{k+1}\|_2 \\ \rho_n^k, & \text{others} \end{cases} \quad (17)$$

Specific steps for ADMM-based distributed optimization between regions are detailed below.

- 1) *Initialization.* The values of the global variables of boundary data are initialized as $\{y_{ij}^0, z_{ij}^0, \forall ij \in L_B\}$ according to the measured data of DN, and the initial values of all Lagrange multipliers are set to 0. Set $k = 0$ and initial value of penalty parameter as ρ^0 ;
- 2) *Intra-regional optimization.* Each regional controller independently solves the optimization problem of (18) and gets the optimal solution of the decision variables $\Gamma := \{P_{dec,j}, Q_{C,j}, Q_{G,j}\}$ as well as the boundary data with the upstream region $B_{up} := \{P_{ab}, Q_{ab}\}$ and the downstream region $B_{dn} := \{P_{cd}^*, Q_{cd}^*\}$. The constraints for intra-regional optimization include (4b), (6), (8), and (10)-(12).

$$\{\Gamma^{k+1}, B_{up}^{k+1}, B_{dn}^{k+1}\} = \arg \min L_n \quad (18)$$

- 3) *Boundary data exchange.* The region n transmits the regional boundary data $B_{up}^{k+1} := \{P_{ab}^{k+1}, Q_{ab}^{k+1}\}$ and $B_{dn}^{k+1} := \{P_{cd}^{*,k+1}, Q_{cd}^{*,k+1}\}$ to region $n-1$ and region $n+1$, and receives $\{P_{ab}^{*,k+1}, Q_{ab}^{*,k+1}\}$ from region $n-1$ and $\{P_{cd}^{k+1}, Q_{cd}^{k+1}\}$ from region $n+1$, respectively.
- 4) *Global variable update.* Based on the received boundary data, each region updates the global variables of boundary data locally by:

$$\begin{cases} y_{ab}^{k+1} = (P_{ab}^{*,k+1} + P_{ab}^{k+1})/2 \\ z_{ab}^{k+1} = (Q_{ab}^{*,k+1} + Q_{ab}^{k+1})/2 \end{cases} \quad (19a)$$

$$\begin{cases} y_{cd}^{k+1} = (P_{cd}^{k+1} + P_{cd}^{*,k+1})/2 \\ z_{cd}^{k+1} = (Q_{cd}^{k+1} + Q_{cd}^{*,k+1})/2 \end{cases} \quad (19b)$$

- 5) *Lagrange multiplier update.* The Lagrange multipliers of boundary data in region n are updated by:

$$\begin{cases} \lambda_{ab}^{P,k+1} = \lambda_{ab}^{P,k} + \rho_n^k (y_{ab}^{k+1} - P_{ab}^{k+1}) \\ \lambda_{ab}^{Q,k+1} = \lambda_{ab}^{Q,k} + \rho_n^k (z_{ab}^{k+1} - Q_{ab}^{k+1}) \end{cases} \quad (20a)$$

$$\begin{cases} \lambda_{cd}^{P*,k+1} = \lambda_{cd}^{P*,k} + \rho_n^k (P_{cd}^{*,k+1} - y_{cd}^{k+1}) \\ \lambda_{cd}^{Q*,k+1} = \lambda_{cd}^{Q*,k} + \rho_n^k (Q_{cd}^{*,k+1} - z_{cd}^{k+1}) \end{cases} \quad (20b)$$

- 6) *Residuals and penalty parameters update.* Each region calculates the primal residual and dual residual of boundary data between regions according to (15) and (16), and then share the boundary data residuals with adjacent regions by distributed communication. Update penalty parameters by (17);
- 7) *Iterative termination judgment.* Set $k = k + 1$, repeat steps (2)-(6) until the infinite norm of the primal residual vector \mathbf{r}^k and the dual residual vector \mathbf{s}^k are both smaller than the predefined threshold δ_d .

B. BBM FOR SVR TAP POSITION

Once ADMM converges, the objective value of f^k and the optimal boundary voltage $U_a, a \in N_B$ of each region are obtained. The boundary data is exchanged as demonstrated in Fig. 2. The ideal SVR tap position \tilde{g} of two adjacent regions can be obtained as:

$$\tilde{g} = \frac{U_a/U_b - 1}{d_{step}} \quad \forall ab \in L_B \quad (21)$$

Specific steps for BBM-based distributed optimization between regions are detailed below.

- 1) *Branch.* Tap position \tilde{g} tends to be a real-value and does not satisfy the integer constraint. Select one \tilde{g}_n , may as well the first one from the substation that does not meet the integer constraints of SVR tap, and construct the following two constraints:

$$g_n \leq [\tilde{g}_n] \quad (22a)$$

$$g_n \geq [\tilde{g}_n] + 1 \quad (22b)$$

where $[\tilde{g}_n]$ is the largest integer that does not exceed \tilde{g}_n . (22a) and (22b) correspond to two different branches of BBM and can be firstly converted into boundary voltage constraints of adjacent regions as (23a), (23b) and (23c), (23d) respectively:

$$u_b \geq u_a^k / (1 + [\tilde{g}_n] \cdot d_{step})^2 \quad (23a)$$

$$u_a \leq u_b^k (1 + [\tilde{g}_n] \cdot d_{step})^2 \quad (23b)$$

$$u_b \leq u_a^k / (1 + ([\tilde{g}_n] + 1) \cdot d_{step})^2 \quad (23c)$$

$$u_a \geq u_b^k (1 - ([\tilde{g}_n] + 1) \cdot d_{step})^2 \quad (23d)$$

Then we add constraints (23a), (23b) and (23c), (23d) to the intra-regional optimization model introduced in portion IV-A respectively and generate two subsequent problems RP1 and RP2, which can be solved

via ADMM. RP1 and RP2 will be branched in a similar way as needed and then continue to solve the subsequent optimization problem until the optimal solution for each integer tap position is obtained.

- 2) *Bound*. Each subproblem is taken as a branch and marked with the result. The minimum objective function value of all subproblems is regarded as a new lower bound and assigned to f_0 . The minimum objective function value of all subproblems that meet the integer constraints of all SVRs is selected as the new upper bound f^* , i.e. $f^* \geq f \geq f_0$.
- 3) *Compare and cut*. Cut off the branch if the optimal objective value is larger than f^* . The other branches that have not been checked are potential branches with optimal solution and defined as unretrieved branches. If f^* has not been got yet, all branches are regarded as unretrieved branches and no branches will be cut. For the unretrieved branches, if the integer constraint of tap position is not satisfied, go back to step 1) until all potential branches have been retrieved. Finally, the optimal integer solution g_n^* of tap position with the smallest objective function value can be realized.

The distributed coordination method proposed in this paper are summarized in Fig. 3, the dashed-line portion indicates the process of ADMM. The cutting plane constraint of (12) is considered after the first iteration ($k \geq 1$) and the global variables, Lagrange multipliers, residuals and penalty parameters are updated by (19), (20), (15)-(16) and (17) respectively to realize the convergence of ADMM. The boundary voltage constraints of (23), constructed by *Branch* process, will be added to the optimization problem and start a new round of iteration if the integer constraints of SVRs have not been satisfied. During the BBM process, the upper bound of the objective function value f^* requires to be obtained before determining whether a branch needs to be cut, which means a feasible solution with the integer constraints of all SVR satisfied are required. Before the upper bound f^* is realized, the branch with the minimum objective function value will be retrieved first to accelerate the search process.

V. CASE STUDIES AND ANALYSIS

A. 32-BUS PRACTICAL CASE

In this paper, a 10kV radial feeder with high penetration of distributed PVs in rural power grid of China is selected to verify the proposed distributed coordination method. In the studied case, as the load is relatively small in rural area, reverse power flow always occurs at noon although the PV installation capacity is not large. According to the historical operation data, a serious overvoltage occurred at 12:30 on November 4, 2016. The net load power of all nodes was 1.23 MW, and the PV active power was about 75% of installed capacity. The outlet voltage of substation is about 1.03 p.u. At that time, the ratio of node voltage higher than 1.05p.u. is up to 64.5% in the network.

The topology of the feeder and the PV distribution are displayed in Fig. 4. The voltage loss rate ΔU^{\max} is set as

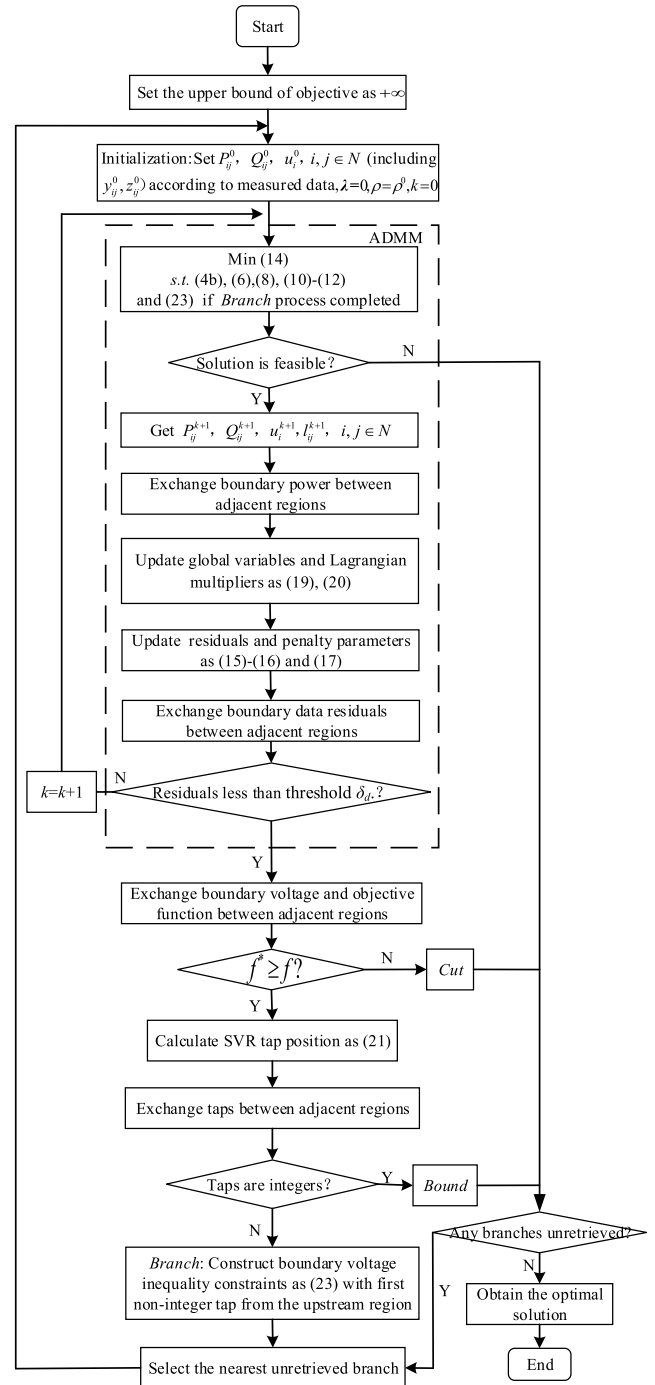


FIGURE 3. Flow chart of the distributed coordination method.

5% here. The voltage of the first node is set as 1.0 p.u. The voltage of node 6 and node 22 are 0.9433 p.u. and 0.9503 p.u. respectively under full load and no PV generation condition. Therefore, two SVRs are installed between node 5/node 6 and node 3/node 22, respectively, partitioning the feeder into three regions. The total capacity of PV units is about 2.22MVA, distributed in 18 nodes. Among them, the PV units in 12 nodes are controllable. There are 4 nodes equipped with RPC devices. The specific parameters

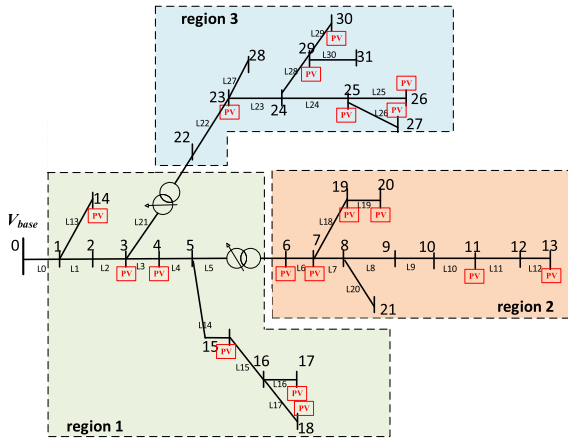


FIGURE 4. Topology of the 32-bus practical case.

TABLE 1. Location and capacity of RPC devices and PV units.

Controllable resources	Location	Capacity (MVA)
RPC devices	7, 13, 17, 27	± 0.1
	4, 18, 19, 29	0.05
PV units	13, 23, 27	0.1
	3, 15, 25	0.2
		0.3
	11, 17	

are listed in Table 1. π_{PV} and π_P are set as ¥800/MW and ¥400/MW. The voltage regulation range of SVR is 32 taps, and the amplitude of each tap is 0.625% of the target voltage. PF_{min} is set as 0.95. The initial penalty parameter is set to $\rho = 10^6$ and the threshold δ_d is set as $10e-6$.

ADMM and BBM are conducted to solve the distributed coordination optimization problem for this system. The solution process is detailed as follows:

- 1) Solving the relaxation problem RP, then the optimal solution of SVR tap of branch 3-22 and 5-6 is obtained as $\tilde{g}^1 = \{\tilde{g}_{1-3}^1, \tilde{g}_{1-2}^1\} = \{-0.3105, 0.3027\}$ with the objective function $f^1 = 11.4639$. According to the condition $g_{1-3} \leq -1$ and $g_{1-3} \geq 0$, RP is decomposed into subproblems RP1 and RP2, and their lower bound f_0 is set as 11.4639.
- 2) Solving the problem RP1 and get the solution of $\tilde{g}^2 = \{-1, -0.1183\}$ and $f^2 = 54.4851$. Solving the problem RP2 and get the solution of $\tilde{g}^3 = \{0, 0.3027\}$ and $f^3 = 11.4691$. Then we have $\min\{f^2, f^3\} = f^3$. As \tilde{g}_{1-2}^3 is real value, the problem RP2 is decomposed into subproblems RP3 and RP4 according to the constraints $g_{1-2} \leq 0$ and $g_{1-2} \geq 1$, and their lower bound is 11.4691.
- 3) Solving the problem RP3, we get $\tilde{g}^4 = \{0, 0\}$ and $f^4 = 36.6984$. Solving the problem RP4, the results are $\tilde{g}^5 = \{0, 1\}$ and $f^5 = 11.5744$, $\min\{f^4, f^5\} = f^5$. \tilde{g}^4 and \tilde{g}^5 are both feasible integer solutions of SVR tap position, so $f^* = 11.5744$ is set as the upper bound.

- 4) As $f^2 > f^*$, there is no need to branch RP1. The optimal solution of SVR tap is $g^* = g^5 = \{0, 1\}$, and the optimal objective value is $f = f^5 = 11.5744$.

The optimal SVR tap position is +1 for region 1-2 and 0 for region 1-3. During the distributed coordination optimization, each region continuously adjusts the output powers of PV units and RPC devices within the region, and finally converge to the global optimal solution. The final APC amount of PV units is 0, and the total RPC amount is 398.1187 kVar. The highest voltage amplitude of the system is 1.05p.u. at node 17 within the limits. The voltage profile is displayed in Fig. 5, which clearly reflects the effectiveness of the proposed method on voltage control.

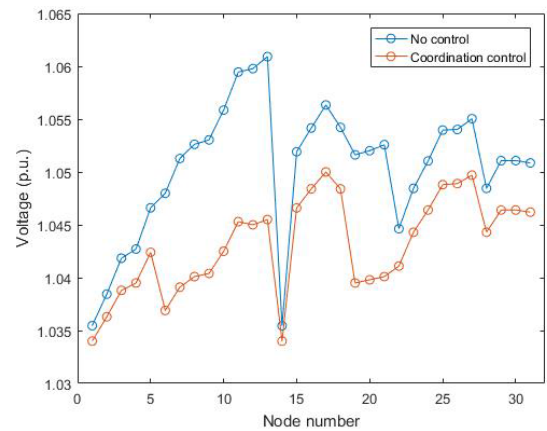


FIGURE 5. Voltage profile of 32-bus practical case.

TABLE 2. Comparison results of centralized optimization and distributed optimization in 32-BUS case.

Control method	Centralized optimization	Distributed optimization
Objective function (¥)	11.5558	11.5744
APC of PV units (kW)	0	0
Reactive power of PV units (kVar)	351.7304	398.1187
Reactive power of RPC (kVar)	381.5035	400
Maximum voltage (p.u./node)	1.05/17	1.05/17
SVR tap (region 1-3/ region 1-2)	0/+1	0/+1
Computational time (s)	6.391	296.918

Comparison results between the proposed distributed optimization method and centralized optimization are listed in Table 2. The performance of the distributed optimization is close to that of centralized optimization. The maximum voltage, APC amount of PV units and SVR tap position are the same with centralized optimization. While the objective, reactive power outputs of PV units and RPC are slightly larger when compared to the centralized optimization, which is caused by the primal and dual residuals. As stated in portion IV-A, if the penalty parameter is not appropriately chosen, convergence may be slow. A tuning technique of

penalty parameter introduced in [10] is utilized in this paper to balance the convergence accuracy and speed, which is denoted as (17).

Comparison results of the proposed method in this paper and the method in [12] are listed in Table 3. The result of [12] is equivalent to the solution of abovementioned RP3. It can be seen from the comparison results that the regional coordination method makes full use of the adjustment advantages of SVR, reduces or even avoids the PV generation losses (0 kW VS 32.5032 kW) and reduces the total cost (¥11.5744 VS ¥36.6984).

TABLE 3. Comparison results with the method of [12] in 32-BUS case.

Control method	This paper	Method of [12]
Objective function (¥)	11.5744	36.6984
APC of PV units (kW)	0	32.5032
Reactive power of PV units (kVar)	398.1187	387.9699
Reactive power of RPC (kVar)	400	400
Maximum voltage (p.u./node)	1.05/17	1.05/11
SVR tap (region1-3/ region 1-2)	0/+1	0/0
Computational time (s)	296.918	96.3

As we can see in Table 2 and Table 3, the computational time of the centralized optimization, the distributed optimization method proposed in [12] and this paper are 6.391s, 96.3s and 296.918s, respectively. The distributed optimization method takes more time to realize converge as an iterative optimization between regions is needed for ADMM. While the computational time of the distributed optimization method proposed in this paper is larger than that proposed in [12] because the BBM also takes time to determine the optimal branch.

B. MODIFIED IEEE 123-BUS CASE

To verify the applicability of the regional distributed coordination method to a large-scale network, a modified IEEE 123-bus system is selected for numerical test, where some nodes are removed and renumbered. The voltage of the first node is set to 1.0 p.u. The voltage of node 14 and node 68 are 0.9585 p.u. and 0.8963 p.u. respectively under full load and no PV generation condition, thus three SVRs are installed on branches 14-19, 14-54, and 62-68. The structure of the DN is illustrated in Fig. 6.

1) OVERVOLTAGE SCENARIO

Assume that the system operates with high PV generation and low load demand situation. As a result, some nodal voltages exceed the upper limit. The voltage of the first node in substation is 1.04p.u. and 12 distributed PV units generation are close to full capacity in a certain scenario. The capacities and installation locations of PV units are listed in Table 4.

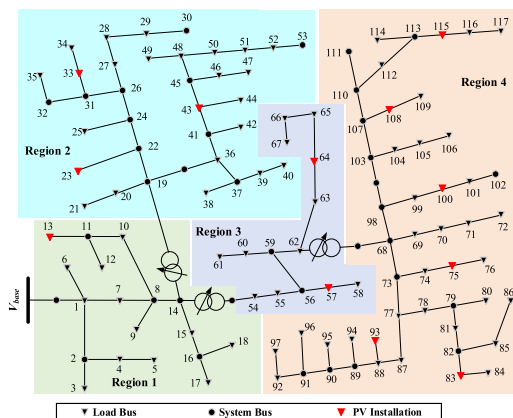


FIGURE 6. Network structure of modified IEEE 123-bus case.

TABLE 4. Locations and capacities of PV units.

Location	Capacity (MVA)
13, 108, 115	0.6
57, 83, 100	0.8
23, 64, 75	1.0
33, 43, 93	1.2

The penalty parameter ρ is set as 100, the other parameters are the same with portion V-A. The solution process is shown in Fig. 7(a) with all the branch trees listed.

After searching four branches, the optimal integer solution of SVR tap position is obtained. The SVR tap positions are +1, +2, and +1 for region 1-2, 1-3, and 3-4, respectively. The voltage control performance is illustrated in Fig. 8(a). The total APC amount of PV units is 28.5364 kW in this situation, and the total reactive power compensation is 836.9341 kVar. The highest voltage is 1.05p.u. at node 13 and node 23, indicating that the voltage limits are satisfied.

Comparison results of centralized optimization and distributed optimization method are listed in Table 5. It is obvious that the performances of the distributed optimization method proposed in this paper are similar to that of centralized optimization, and the error is small enough to be negligible. The network maximum voltage and SVR tap position of distributed optimization are the same with those of centralized optimization, while the objective and APC amount of PV units, the reactive power output of PV units are slightly larger/smaller than centralized optimization, respectively. The difference is mainly due to the convergence accuracy.

Comparison results with the method proposed in [12] are listed in Table 6. It can be seen that the APC amount, reactive power output of PV units and the total cost are highly reduced by the proposed method in this paper. The SVR tap action changes the power flow distribution, thus the highest voltage position of the network is different.

The computational time of the distributed optimization method proposed in this paper increases significantly with the expansion of the network scale. The problem is solved

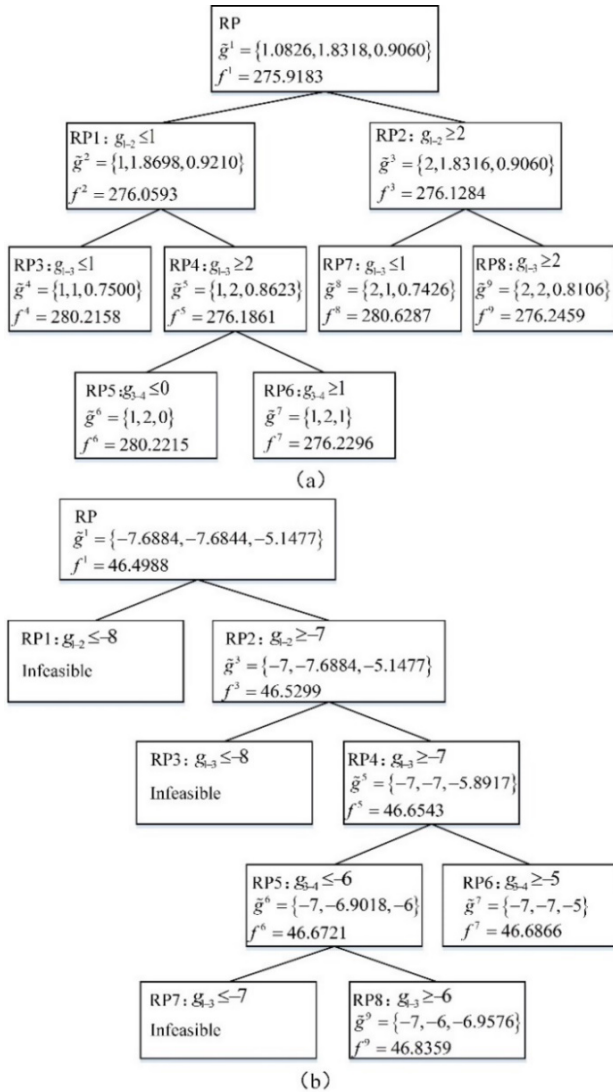


FIGURE 7. Solution process of modified IEEE 123-bus case. (a) Overvoltage scenario, (b) low voltage scenario.

by IBM CPLEX in MATLAB R2013a environment, and the computational time can be reduced significantly by parallel computing of multiple regional controllers in practical applications.

2) LOW VOLTAGE SCENARIO

The traditional long-feeder distribution network is prone to the problem that the feeder voltage may lower than the lower limit when the load is heavy and no PV generation at night. In a certain scenario, the voltage of the first node is 1.04p.u. and the voltages of some nodes are lower than the lower limit 0.95p.u., as shown in Fig. 8(b). In this situation, the voltage profile can be improved by adjusting the SVR. The solution process is shown in Fig. 7(b).

After searching four branches, the optimal integer solution of SVR tap position is obtained. The SVR tap positions are -7 , -7 , and -5 for region 1-2, 1-3, and 3-4, respectively.

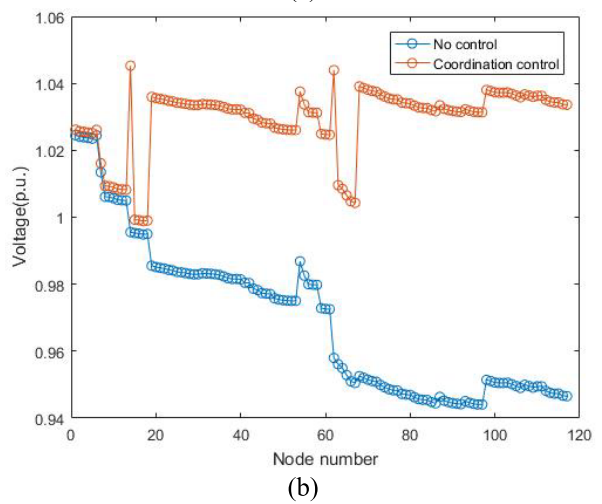
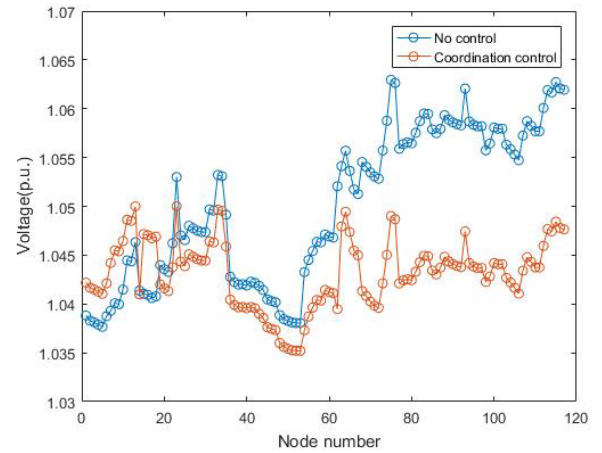


FIGURE 8. Voltage profile of modified IEEE 123-bus case. (a) Overvoltage scenario, (b) low voltage scenario.

TABLE 5. comparison results of centralized optimization and distributed optimization of 123-BUS case in overvoltage scenario.

Control method	Centralized optimization	Distributed optimization
Objective function (¥)	276.2279	276.2296
Reactive power of PV units (kVar)	839.577	836.9341
APC of PV units (kW)	28.3993	28.5364
Maximum voltage (p.u./node)	1.05/13/23	1.05/13/23
SVR tap (region 1-2/ region 1-3/ region 3-4)	+1/+2/+1	+1/+2/+1
Computational time (s)	37.341	1851.348

The voltage profile is significantly improved as presented in Fig. 8(b). The voltage varies significantly at the regional boundary and the voltage mutation is caused by SVR taps action.

Table 7 summarizes the comparison results of the proposed distributed coordination optimization method with the centralized optimization. Similar to the overvoltage scenario, the regional distributed coordination optimization

TABLE 6. Comparison results with the method of [12] in 123-BUS case.

Control method	This paper	Method of [12]
Objective function (¥)	276.2296	312.6085
Reactive power of PV units (kVar)	839.577	1221.1
APC of PV units (kW)	28.5364	63.6435
Maximum voltage (p.u./node)	1.05/13/23	1.05/23/75
SVR tap (region 1-2/ region 1-3/ region 3-4)	+1/+2/+1	0/0/0
Computational time (s)	1851.348	177.9

TABLE 7. Comparison results of centralized optimization and distributed optimization of 123-BUS case in low voltage scenario.

Control method	Centralized optimization	Distributed optimization
Objective function (¥)	46.6860	46.6866
Minimum voltage (p.u./node)	0.9990/18	0.9990/18
SVR tap (region 1-2/ region 1-3/ region 3-4)	-7/-7/-5	-7/-7/-5
Computational time (s)	10.155	768.822

can achieve almost the same performance with centralized optimization and ensure the control precision.

VI. CONCLUSION

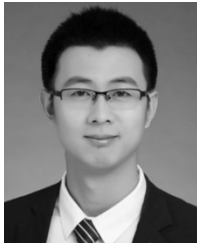
To deal with the voltage violation problem in long-feeder DN with high penetration of PV, this paper utilizes network characteristics to configure SVRs and establishes a fully distributed optimization model to minimize the total cost of network losses and PV generation losses. ADMM and BBM are combined and employed to handle the inter-regional coordination and nonconvex problem introduced by SVR tap position. The simulation results of a practical 32-bus system and a modified IEEE 123-bus system indicate that the proposed method can mitigate the low voltage problem on heavy load condition as well as the overvoltage problem caused by high penetration of PV. The control performance is very close to that of centralized optimization in a distributed manner. Furthermore, the SVR tap action can reduce or even avoid PV generation losses, thus reducing the total cost and improving the PV permeability rate.

REFERENCES

- [1] A. Keane, L. F. Ochoa, E. Vittal, C. J. Dent, and G. P. Harrison, "Enhanced utilization of voltage control resources with distributed generation," *IEEE Trans. Power Syst.*, vol. 26, no. 1, pp. 252–260, Feb. 2011.
- [2] S. Uddin, O. Krause, and D. Martin, "Energy management for distribution networks through capacity constrained state optimization," *IEEE Access*, vol. 5, pp. 21743–21752, 2017.
- [3] X. Dou *et al.*, "A distributed voltage control strategy for multi-microgrid active distribution networks considering economy and response speed," *IEEE Access*, vol. 6, pp. 31259–31268, 2018.
- [4] X. Zhu, H. Han, Q. Shi, H. Cui, G. Zu, and S. Gao, "A multi-stage optimization approach for active distribution network scheduling considering coordinated electrical vehicle charging strategy," *IEEE Access*, vol. 6, pp. 50117–50130, 2018.

- [5] S. Chen, W. Hu, and Z. Chen, "Comprehensive cost minimization in distribution networks using segmented-time feeder reconfiguration and reactive power control of distributed generators," *IEEE Trans. Power Syst.*, vol. 31, no. 2, pp. 983–993, Mar. 2016.
- [6] D. Zhang, Z. Fu, and L. Zhang, "Joint optimization for power loss reduction in distribution systems," *IEEE Trans. Power Syst.*, vol. 23, no. 1, pp. 161–169, Feb. 2008.
- [7] H. Ahmadi, J. R. Martí, and H. W. Dommel, "A framework for volt-VAR optimization in distribution systems," *IEEE Trans. Smart Grid*, vol. 6, no. 3, pp. 1473–1483, May 2015.
- [8] B. Kocuk, S. S. Dey, and X. A. Sun, "New formulation and strong MISOCP relaxations for AC optimal transmission switching problem," *IEEE Trans. Power Syst.*, vol. 32, no. 6, pp. 4161–4170, Nov. 2017.
- [9] Z. Tian, W. Wu, B. Zhang, and A. Bose, "Mixed-integer second-order cone programming model for VAR optimization and network reconfiguration in active distribution networks," *IET Gener. Transmiss. Distrib.*, vol. 10, no. 8, pp. 1938–1946, May 2016.
- [10] W. Zheng, W. Wu, B. Zhang, H. Sun, and Y. Liu, "A fully distributed reactive power optimization and control method for active distribution networks," *IEEE Trans. Smart Grid*, vol. 7, no. 2, pp. 1021–1033, Mar. 2016.
- [11] P. Lulc, S. Backhaus, and M. Chertkov, "Optimal distributed control of reactive power via the alternating direction method of multipliers," *IEEE Trans. Energy Convers.*, vol. 29, no. 4, pp. 968–977, Dec. 2014.
- [12] Y. Chai, L. Guo, C. Wang, Z. Zhao, X. Du, and J. Pan, "Network partition and voltage coordination control for distribution networks with high penetration of distributed PV units," *IEEE Trans. Power Syst.*, vol. 33, no. 3, pp. 3396–3407, May 2018.
- [13] P. Li *et al.*, "Optimal operation of soft open points in active distribution networks under three-phase unbalanced conditions," *IEEE Trans. Smart Grid*, vol. 10, no. 1, pp. 380–391, Jan. 2019.
- [14] E. Dall'Anese, H. Zhu, and G. B. Giannakis, "Distributed optimal power flow for smart microgrids," *IEEE Trans. Smart Grid*, vol. 4, no. 3, pp. 1464–1475, Sep. 2013.
- [15] M. Farivar, C. R. Clarke, K. M. Chandy, and S. H. Low, "Inverter VAR control for distribution systems with renewables," in *Proc. IEEE Int. Conf. Smart Grid Commun.*, Oct. 2011, pp. 457–462.
- [16] M. Farivar and S. H. Low, "Branch flow model: Relaxations and convexification—Part I," *IEEE Trans. Power Syst.*, vol. 28, no. 3, pp. 2554–2564, Aug. 2013.
- [17] S. Y. Abdelouadoud, R. Girard, T. Guiot, and F. P. Neirac, "Optimal power flow of a distribution system based on increasingly tight cutting planes added to a second order cone relaxation," *Int. J. Elect. Power Energy Syst.*, vol. 69, pp. 9–17, Jul. 2015.
- [18] H. Gao, J. Liu, and L. Wang, "Cutting planes based relaxed optimal power flow in active distribution systems," *Electr. Power Syst. Res.*, vol. 143, pp. 272–280, Feb. 2017.
- [19] I. Lobel and A. Ozdaglar, "Distributed subgradient methods for convex optimization over random networks," *IEEE Trans. Autom. Control*, vol. 56, no. 6, pp. 1291–1306, Jun. 2011.
- [20] A. Nedic, A. Ozdaglar, and P. A. Parrilo, "Constrained consensus and optimization in multi-agent networks," *IEEE Trans. Autom. Control*, vol. 55, no. 4, pp. 922–938, Apr. 2010.
- [21] G. Shi, K. H. Johansson, and Y. Hong, "Reaching an optimal consensus: Dynamical systems that compute intersections of convex sets," *IEEE Trans. Autom. Control*, vol. 58, no. 3, pp. 610–622, Mar. 2013.
- [22] Y. Lou, G. Shi, K. H. Johansson, and Y. Hong, "Approximate projected consensus for convex intersection computation: Convergence analysis and critical error angle," *IEEE Trans. Autom. Control*, vol. 59, no. 7, pp. 1722–1736, Jul. 2014.
- [23] W. Shi, Q. Ling, K. Yuan, G. Wu, and W. Yin, "On the linear convergence of the ADMM in decentralized consensus optimization," *IEEE Trans. Signal Process.*, vol. 62, no. 7, pp. 1750–1761, Apr. 2014.
- [24] V. Kekatots and G. B. Giannakis, "Distributed robust power system state estimation," *IEEE Trans. Power Syst.*, vol. 28, no. 2, pp. 1617–1626, May 2013.
- [25] Q. Liu and J. Wang, "A second-order multi-agent network for bound-constrained distributed optimization," *IEEE Trans. Autom. Control*, vol. 60, no. 12, pp. 3310–3315, Dec. 2015.
- [26] W. Shi, Q. Ling, G. Wu, and W. Yin, "EXTRA: An exact first-order algorithm for decentralized consensus optimization," *SIAM J. Optim.*, vol. 25, no. 2, pp. 944–966, Apr. 2014.
- [27] J. Lei, H.-F. Chen, and H.-T. Fang, "Primal-dual algorithm for distributed constrained optimization," *Syst. Control Lett.*, vol. 96, pp. 110–117, Oct. 2016.

- [28] B. Zhao, Z. Xu, C. Xu, C. Wang, and F. Lin, "Network partition-based zonal voltage control for distribution networks with distributed PV systems," *IEEE Trans. Smart Grid*, vol. 9, no. 5, pp. 4087–4098, Sep. 2018.
- [29] E. Cotilla-Sanchez, P. D. H. Hines, C. Barrows, S. Blumsack, and M. Patel, "Multi-attribute partitioning of power networks based on electrical distance," *IEEE Trans. Power Syst.*, vol. 28, no. 4, pp. 4979–4987, Nov. 2013.



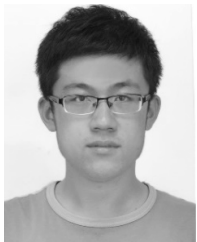
YIXIN LIU received the B.S. and Ph.D. degrees in electrical engineering from Tianjin University, Tianjin, China, in 2013 and 2018, respectively, where he is currently an Assistant Professor with the School of Electrical and Information Engineering.

His research interests include the distribution system analysis and planning, energy management system of microgrid, and electricity power market.



LI GUO (M'11) received the B.S. and Ph.D. degrees in electrical engineering from the South China University of Technology, Guangzhou, China, in 2002 and 2007, respectively.

From 2007 to 2009, he was a Postdoctoral Research Fellow with Tianjin University, Tianjin, China, where he has been a Professor, since 2016. His current research interests include optimal planning and design of microgrid, the coordinated operating strategy of microgrid, and the advanced energy management systems.



CHANG LU received the B.S. degree in electrical engineering from Tianjin University, Tianjin, China, in 2016, where he is currently pursuing the M.S. degree.

His current research interest includes operation of distribution networks and microgrids with high penetration of distributed photovoltaic.



YUANYUAN CHAI received the B.S. degree in electrical engineering from Tianjin University, Tianjin, China, in 2015, where she is currently pursuing the Ph.D. degree.

Her current research interests include renewable energy management and power quality improvement in active distribution networks.



SHUANG GAO (M'14) received the B.S. degree in electrical engineering from Tianjin University, in 2007, and the Ph.D. degree from The University of Hong Kong, in 2014.

In 2014, she joined the Department of Electrical Engineering, Tianjin University, as an Assistant Professor, and was also a part-time Research Associate in Hong Kong and The Hong Kong Polytechnic University, in 2014 and 2015. Her current research interests include integration of renewables and electric vehicles into the power networks, demand side response, and electrified transportation systems.



Bin Xu is currently a Senior Engineer with the Institute of Electric Power Research, Anhui, China.

His current research interests include power quality analysis and the control technology of power grids.

...